HHS Public Access

Author manuscript

Nature. Author manuscript; available in PMC 2016 November 02.

Published in final edited form as:

Nature. ; 534(7606): 200–205. doi:10.1038/nature17993.

The genetic history of Ice Age Europe

A full list of authors and affiliations appears at the end of the article.

Abstract

Modern humans arrived in Europe ~45,000 years ago, but little is known about their genetic composition before the start of farming ~8,500 years ago. We analyze genome-wide data from 51 Eurasians from ~45,000-7,000 years ago. Over this time, the proportion of Neanderthal DNA decreased from 3–6% to around 2%, consistent with natural selection against Neanderthal variants in modern humans. Whereas the earliest modern humans in Europe did not contribute substantially to present-day Europeans, all individuals between ~37,000 and ~14,000 years ago descended from a single founder population which forms part of the ancestry of present-day Europeans. A ~35,000 year old individual from northwest Europe represents an early branch of this founder population which was then displaced across a broad region, before reappearing in southwest Europe during the Ice Age ~19,000 years ago. During the major warming period after ~14,000 years ago, a new genetic component related to present-day Near Easterners appears in Europe. These results document how population turnover and migration have been recurring themes of European pre-history.

Modern humans arrived in Europe around 45,000 years ago and have lived there ever since, even during the Last Glacial Maximum 25,000-19,000 years ago when large parts of Europe were covered in ice[1]. A major question is how climatic fluctuations influenced the population history of Europe and to what extent changes in material cultures documented by archaeology and correlating to climatic events corresponded to movements of people. To date, it has been difficult to address this question because genome-wide ancient DNA has been retrieved from just five Upper Paleolithic individuals in Eurasia[2–4]. Here we assemble and analyze genome-wide data from 51 modern humans dating from 45,000 to 7,000 years ago (Table 1; Extended Data Table 1; Supplementary Information section 1).

Correspondence and requests for materials should be addressed to David Reich (reich@genetics.med.harvard.edu).

*These authors contributed equally

+These authors co-supervised the study

Author Contributions

JKr, SP and DR conceived the idea for the study. QF, CP, MH, WH, MMe, VSlo, RGC, APD, ND, VSla, AT, FM, BG, EV, MRG, LGS, CN-M, MT-N, SC, OTM, SB, MPer, DCo, MLa, SR, AR, FV, CT, KW, DG, HR, IC, DFl, PSe, MAM, CC, HB, NJC, KH, VM, DGD, JS, DCa, RP, JKr, SP and DR assembled archaeological material. QF, CP, MH, DFe, AF, WH, MMe, AM, BN, NR, VSlo, ST, HB, DGD, MPR, RP, JKr, SP and DR performed or supervised wet laboratory work. QF, CP, MH, MPet, SM, AP, IL, MLi, IM, SS, PSk, JKe, NP and DR analyzed data. QF, CP, MH, MPet, JKe, SP and DR wrote the manuscript and supplements.

The aligned sequences are available through the European Nucleotide Archive under accession number PRJEB13123.

The authors declare no competing financial interests.

Readers are welcome to comment on the online version of the paper.

Ancient DNA data

We extracted DNA from human remains in dedicated clean rooms[5], and transformed the extracts into Illumina sequencing libraries[6–8]. A major challenge in ancient DNA research is that the vast majority of the DNA extracted from most specimens is of microbial origin, making random shotgun sequencing prohibitively expensive. We addressed this problem by enriching the libraries for between 390,000 and 3.7 million single nucleotide polymorphisms (SNPs) in the nuclear genome via hybridizing to pools of previously synthesized 52-base-pair oligonucleotide probes targeting these positions (this strategy makes it possible to generate genome-wide data from samples with high percentages of microbial DNA that are not practical to study by shotgun sequencing)[3,9]. We sequenced the isolated DNA fragments from both ends, and mapped the consensus sequences to the human genome (*hg19*), retaining fragments that overlapped the targeted SNPs. After removing fragments with identical start and end positions to eliminate duplicates produced during library amplification, we chose one fragment at random to represent each individual at each SNP.

Contamination from present-day human DNA is a danger in ancient DNA research. To address this we took advantage of three characteristic features of ancient DNA (Supplementary Information section 2). First, for an uncontaminated specimen, we expect only a single mitochondrial DNA sequence to be present, allowing us to detect contamination as a mixture of mitochondrial sequences. Second, because males carry a single X chromosome, we can detect contamination in male specimens as polymorphisms on chromosome X[10]. Third, cytosines at the ends of genuine ancient DNA molecules are often deaminated, resulting in apparent cytosine to thymine substitutions[11]. Thus, restricting analysis to molecules with evidence of such deamination filters out the great majority of contaminating molecules[12]. For libraries from males with evidence of mitochondrial DNA contamination or X chromosomal contamination estimates >2.5%—as well as for all libraries from females—we restricted the analyses to sequences with evidence of cytosine deamination (Supplementary Information section 2). After merging libraries from the same individual and limiting to individuals with >4,000 targeted SNPs covered at least once, 38 individuals remained, which we merged with newly generated shotgun sequencing data from the *Karelia* individual[9] (2.0-fold coverage), and published data from ancient[2–4,7,13–19] and present-day humans[20]. The final dataset includes 51 ancient modern humans, of which 16 had at least 790,000 SNPs covered (Figure 1; Table 1; Extended Data Table 1).

Natural selection has reduced Neanderthal ancestry over the last 45,000 years

We used two previously published statistics[3,7,21] to ask if the proportion of Neanderthal ancestry in Eurasians changed over the last 45,000 years. Whereas on the order of 2% of present-day Eurasian DNA is of Neanderthal origin (Extended Data Table 2), the ancient modern human genomes carry significantly more Neanderthal DNA (Figure 2) ($P \ll 10^{-12}$). Using one statistic, we estimate a decline from 4.3–5.7% from a time shortly after introgression to 1.1–2.2% in Eurasians today (Figure 2). Using the other statistic, we estimate a decline from 3.2–4.2% to 1.8–2.3% (Extended Data Figure 1, Extended Data

Table 3). Because all the European samples we analyzed dating to between 37,000 and 14,000 years ago are consistent with descent from a single founding population, admixture with populations with lower Neanderthal ancestry cannot explain the steady decrease in Neanderthal-derived DNA that we detect during this period, showing that natural selection against Neanderthal DNA must have driven this phenomenon (Figure 2). We also obtain an independent line of evidence for selection from our observation that the decrease in Neanderthal-derived alleles is more marked near genes than in less constrained regions of the genome (P=0.010) (Supplementary Information section 3; Extended Data Table 3)[22–25].

Y chromosomes, mitochondrial DNA and phenotypically important mutations

We used the proportion of sequences mapping to the Y chromosome to infer sex (Extended Data Table 4; Supplementary Information section 4), and determined Y chromosome haplogroups for the males. We were surprised to find haplogroup R1b in the ~14,000-year-old *Villabruna* individual from Italy. While the predominance of R1b in western Europe today is owes its origin to Bronze Age migrations from the eastern European steppe[9], its presence in *Villabruna* and in a ~7,000-year-old farmer from Iberia[9] document a deeper history of this haplotype in more western parts of Europe. Additional evidence of an early link between west and east comes from the *HERC2* locus, where a derived allele that is the primary driver of light eye color in Europeans appears nearly simultaneously in specimens from Italy and the Caucasus ~14,000-13,000 years ago. Extended Data Table 5 presents results for additional alleles of known phenotypic importance. When analyzing the mitochondrial genomes we note the presence of haplogroup M in a ~27,000-year-old individual from southern Italy (*Ostuni1*) in agreement with the observation that this haplogroup, which today occurs in Asia and is absent in Europe, was present in pre-Last Glacial Maximum Europe and became lost during the Ice Age[26]. We also find that the ~33,000 year old *Muierii2* from Romania carries a basal version of haplogroup U6, in agreement with the hypothesis that the presence of derived versions of this haplogroup in North Africans today is due to back-migration from western Eurasia[27].

Genetic clustering of the ancient specimens

This dataset provides an unprecedented opportunity to study the population history of Upper Paleolithic Europe over more than 30,000 years. In order to not prejudice any association between genetic and archaeological groupings among the individuals studied, we first allowed the genetic data alone to drive the groupings of the specimens and only afterward examined their associations with archaeological cultural complexes. We began by computing *f3*-statistics[14] of the form *f3(X, Y; Mbuti)*, which measure shared genetic drift between a pair of ancient individuals after divergence from an outgroup (here *Mbuti* from sub-Saharan Africa), which allowed us to observe clear clusters of samples (Figure 3A; Extended Data Figure 2). Through Multi-Dimensional Scaling (MDS) analysis of this matrix (Figure 3B), as well as through *D*-statistic analyses[28] (Supplementary Information section 5), we identified five clusters of individuals with substantial shared genetic drift, which we name after the oldest individual with >1.0-fold coverage in each cluster (Supplementary

Information section 5; Table 1; Extended Data Table 1). In contrast, we were not able to identify clear structure among these samples based on model-based clustering[29,30], which may reflect the fact that many of the samples are so ancient that present-day patterns of human variation are not very relevant to understanding their patterns of genetic differentiation[4,13]. The "Vestonice Cluster" is composed of 14 pre-Ice Age individuals from 34,000-26,000 years ago, who are all associated with the archaeologically defined Gravettian culture. The "Mal'ta Cluster" is composed of three individuals from the Glacial Maximum 24,000-17,000 years ago from the Lake Baikal region of Siberia. The "El Mirón Cluster" is composed of 6 Late Glacial individuals from 19,000-14,000 years ago, who are all associated with the Magdalenian culture. The "Villabruna Cluster" is composed of 13 post-Ice Age individuals from 14,000-7,000 years ago, associated with the Azilian, Epipaleolithic and Mesolithic cultures. The "Satsurblia Cluster" is composed of two individuals from 13,000-10,000 years ago from the northern Caucasus[2]. There were ten samples that we did not assign to any cluster, either because of evidence of representing distinct early lineages, (*Ust'-Ishim, Oase1, Kostenki14*, *GoyetQ116*-1, *Muierii2, Cioclovina1, Kostenki12*), or because they were admixed between major clusters (*Karelia* or *Motala12*), or of very different ancestry (*Stuttgart*). To classify the ancestry of additional low coverage samples, we built an admixture graph that fits the allele frequency correlation patterns among high coverage samples[28] (Supplementary Information section 6; Figure 4a). We fit each low coverage sample into the graph in turn, including all fragments from every individual rather than just ones with evidence of cytosine deamination, accounting for contamination bias by modeling (Supplementary Information section 7).

A single founding population during most of the Upper Paleolithic period in Europe

Prior to this work, the most ambitious genetic analysis of early modern humans in Europe was based on the ~37,000-year-old *Kostenki14*[4]. That analysis suggested that the population to which *Kostenki14* belonged harbored within it the three major lineages that exist in mixed form in Europe today[15]: (1) a lineage related to all later pre-Neolithic Europeans, (2) a "Basal Eurasian" lineage that split from the ancestors of Europeans and East Asians before they separated from each other; and (3) a lineage related to the ~24,000-year-old *Mal'ta1* from Siberia. With our more extensive sampling of Ice Age Europe, we find no support for this model. When we test whether the ~45,000-year-old *Ust'-Ishim* – an early Eurasian without any evidence of Basal Eurasian ancestry – shares more alleles with one test individual or another by computing statistics of the form *D(Test1, Test2; Ust'-Ishim, Mbuti)*, we find that the statistic is consistent with zero when the *Test* populations are any pre-Neolithic Europeans or present-day East Asians[3,13,31]. This would not be expected if some of the pre-Neolithic Europeans, including *Kostenki14,* had Basal Eurasian ancestry (Supplementary Information section 8). We also find no evidence for the suggestion that the *Mal'ta1* lineage contributed to Upper Paleolithic Europeans[4], because when we compute the statistic *D(Test1, Test2; Mal'ta1, Mbuti),* we find that the statistic is consistent with zero when the *Test* populations are any pre-Neolithic Europeans beginning with *Kostenki14*, implying descent from a single founder population since separation from the lineage leading to *Mal'ta1* (Supplementary Information section 9). A corollary of this finding is that the

widespread presence of *Mal'ta1*-related ancestry in present-day Europeans[15] is due to migrations from the Eurasian steppe in the Neolithic and Bronze Age periods[9]; it is not due to population structure within pre-Neolithic Europe as proposed in the initial analysis of the *Kostenki14* genome[4].

Resurgence of an early branching European lineage during the Last Glacial Maximum

Among the newly reported individuals, *GoyetQ116-1* from present-day Belgium is the oldest at ~35,000 years ago. It is similar to the ~37,000 year old *Kostenki14* and all later samples in that it shares more alleles with present-day Europeans (*e.g. French*) than with East Asians (*e.g. Han*). In contrast, *Ust'-Ishim* and *Oase1*, which predate *GoyetQ116-1* and *Kostenki14,* do not show any distinctive affinity to later Europeans (Extended Data Table 6). Thus, from at least about 37,000 years ago, populations in Europe shared at least some ancestry with present Europeans. However, *GoyetQ116-1* differs from *Kostenki14* and from all individuals of the succeeding Vestonice Cluster in that both *f3*-statistics (Figure 3; Extended Data Figure 2) and *D*-statistics show that it shares more alleles with members of the El Mirón Cluster who lived 19,000-14,000 years ago than with other pre-Neolithic Europeans (Supplementary Information section 10). Thus, *GoyetQ116-1* has affinity to individuals who lived more than fifteen thousand years later. While at least half of the ancestry of all El Mirón Cluster individuals comes from the *GoyetQ116-1* cluster, this proportion varies, with the largest amount in individuals outside Iberia ($Z=-4.8$) (Supplementary Information section 10).

A drawing together of the ancestry of Europe and the Near East after ~14,000 years ago

Beginning around 14,000 years ago with the Villabruna Cluster, the strong affinity to *GoyetQ116-1* seen in El Mirón Cluster individuals who belong the Late Glacial Magdalenian Culture is greatly attenuated (Supplementary Information section 10). To test if this change might reflect gene flow from populations that did not descend from the >37,000 year old European founder population, we computed statistics of the form *D(Early European, Later European; Y, Mbuti*) where *Y* are various present-day non-Africans. If no gene flow from exogenous populations occurred, this statistic is expected to be zero. Figure 4b shows that it is consistent with zero ($|Z|<3$) for nearly all individuals dating to between about 37,000 and 14,000 years ago. However, beginning with the Villabruna Cluster, it becomes highly significantly negative in comparisons where the non-European population (*Y*) is Near Easterners (Figure 4b; Extended Data Figure 3; Supplementary Information section 11). This must reflect gene flow into the Villabruna Cluster from a population related to present-day Near Easterners rather than gene flow in the reverse direction, because we do not see similar patterns in earlier Europeans although they share substantial amounts of their ancestry with the Villabruna Cluster (Figure 4b). The "Satsurblia Cluster" individuals from the Caucasus dating to ~13,000-10,000 years ago[2] share more alleles with the Villabruna Cluster individuals than they do with earlier Europeans, indicating that they are related to the population that contributed new alleles to people in the Villabruna Cluster, although they

cannot be the direct source of the gene flow, among other reasons because they have large amounts of Basal Eurasian ancestry while Villabruna Cluster individuals do not[2] (Supplementary Information section 12; Extended Data Figure 4). One possible explanation for the sudden drawing together of the ancestry of Europe and the Near East at this time is long-distance migrations from the Near East into Europe. However, a plausible alternative is population structure, whereby Upper Paleolithic Europe harbored multiple groups that differed in their relationship to the Near East, with the balance shifting among groups as a result of demographic changes after the Ice Age.

The Villabruna Cluster includes the largest group of samples in this study. This allows us to study heterogeneity within this cluster (Supplementary Information section 13). First, we detect differences in the degree of allele sharing with members of the El Mirón Cluster, as revealed by significant statistics of the form *D(Test1, Test2; El Mirón Cluster, Mbuti)*. Second, we detect an excess of allele sharing with East Asians in a subset of Villabruna Cluster individuals - beginning with a ~13,000 year old sample from Switzerland - as revealed by significant statistics of the form *D(Test1, Test2; Han, Mbuti)* (Figure 4b and Extended Data Figure 3). For example, *Han* Chinese share more alleles with two Villabruna Cluster individuals (*Loschbour* and *LaBrana1*) than they do with *Kostenki14*, as reflected in significantly negative statistics of the form *D(Kostenki14, Loschbour/LaBrana1; Han, Mbuti)*[4]. This statistic was originally interpreted as evidence of Basal Eurasian ancestry in *Kostenki14*. However, because this statistic is consistent with zero when *Han* is replaced with *Ust'-Ishim*, these findings cannot be driven by Basal Eurasian ancestry (as we also discuss above), and must instead be driven by gene flow between populations related to East Asians and the ancestors of some Europeans (Supplementary Information section 8).

Conclusions

We have shown that the population history of pre-Neolithic Europe was complex in several respects. First, at least some of the initial modern humans to appear in Europe, exemplified by *Ust'-Ishim* and *Oase1*, failed to contribute appreciably to the current European gene pool. Only from around 37,000 years ago do all the European individuals analyzed share ancestry with present-day Europeans[3]. Second, from the time of *Kostenki14* about 37,000 years ago until the time of the Villabruna Cluster about 14,000 years ago, all individuals seem to derive from a single ancestral population with no evidence of substantial genetic influx from elsewhere. It is interesting that during this time, the Mal'ta Cluster is not represented in any of the individuals we sampled from Europe. Thus, while individuals assigned to the Gravettian cultural complex in Europe are associated with the Vestonice Cluster, there is no genetic connection between them and the *Mal'ta1* individual in Siberia despite the fact that Venus figurines are associated with both. This suggests that if this similarity is not a coincidence[32], it reflects diffusion of ideas rather than movements of people. Third, we find that *GoyetQ116-1* derives from a different deep branch of the European founder population than the Vestonice Cluster which became predominant in many places in Europe between 34,000 and 26,000 years ago including at Goyet Cave. *GoyetQ116-1* is chronologically associated with the Aurignacian cultural complex. Thus, the subsequent spread of the Vestonice Cluster, which is associated with the Gravettian cultural complex, shows that the spread of the latter culture was mediated at least in part by population movements. Fourth,

the population represented by *GoyetQ116-1* did not disappear, as its descendants became widespread again after ~19,000 years ago in the El Mirón Cluster when we detect them in Iberia. The El Mirón Cluster is associated with the Magdalenian culture and may represent a post-ice age expansion from southwestern European refugia[33]. Fifth, beginning with the Villabruna Cluster at least ~14,000 years ago, all European individuals analyzed show an affinity to the Near East. This correlates in time to the Bølling-Allerød interstadial, the first significant warming period after the Ice Age[34]. Archaeologically, it correlates with cultural transitions within the Epigravettian in Southern Europe[35] and the Magdalenian-to-Azilian transition in Western Europe[36]. Thus, the appearance of the Villabruna Cluster may reflect migrations or population shifts within Europe at the end of the Ice Age, an observation that is also consistent with the evidence of turnover of mitochondrial DNA sequences at this time[26,37]. One scenario that could explain these patterns is a population expansion from southeastern European or west Asian refugia after the Ice Age, drawing together the genetic ancestry of Europe and the Near East. Sixth, within the Villabruna Cluster, some, but not all, individuals have affinity to East Asians. An important direction for future work is to generate similar ancient DNA data from southeastern Europe and the Near East to arrive at a more complete picture of the Upper Paleolithic population history of western Eurasia[38].

Extended Data

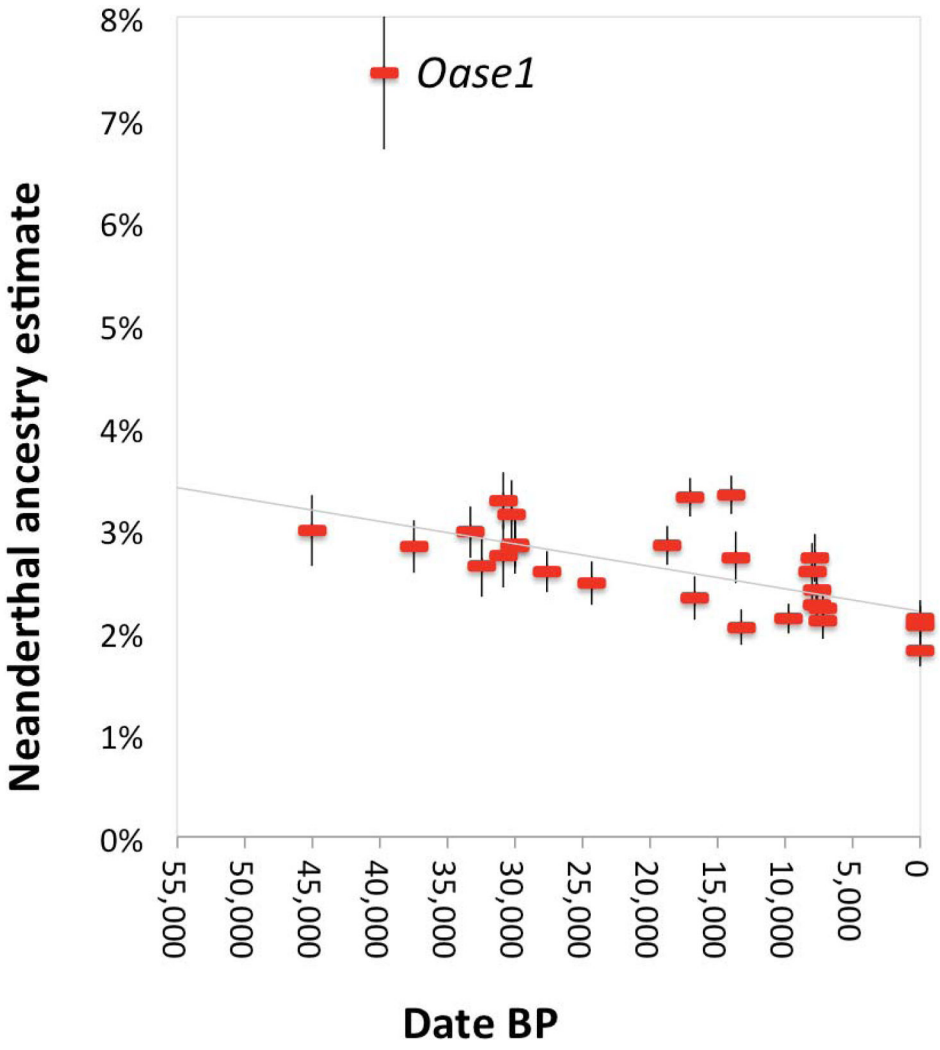

Extended Data Figure 1. A decrease in Neanderthal ancestry in the last 45,000 years

This is similar to Figure 2, except we use ancestry estimates from rates of alleles matching to Neanderthal rather than f_4-ratios, as described in Supplementary Information section 3). The least squares fit excludes *Oase1* (as an outlier with recent Neanderthal ancestry) and Europeans (known to have reduce Neanderthal ancestry). The regression slope is significantly negative (P=0.00004, Extended Data Table 3).

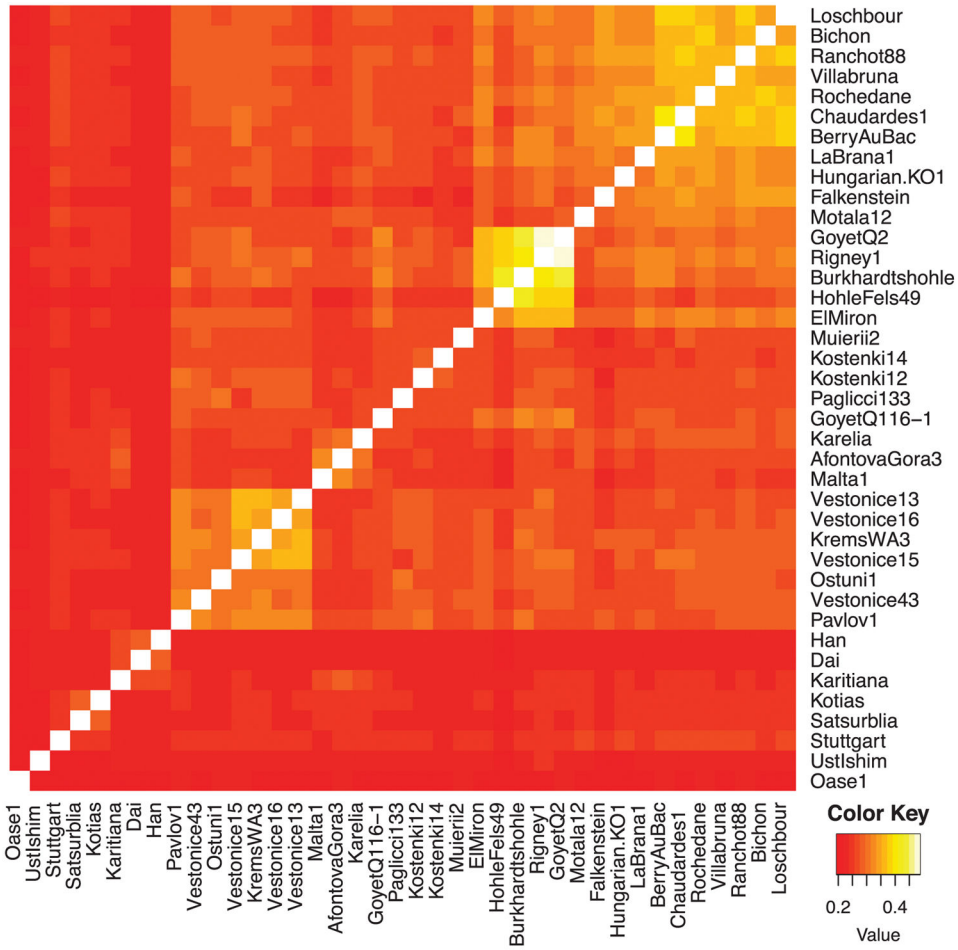

Extended Data Fig. 2. Heat matrix of pairwise f_3(*X, Y; Mbuti*) for selected ancient samples
We analyze only samples with at least 30,000 SNPs covered at least once, which pass our quality control.

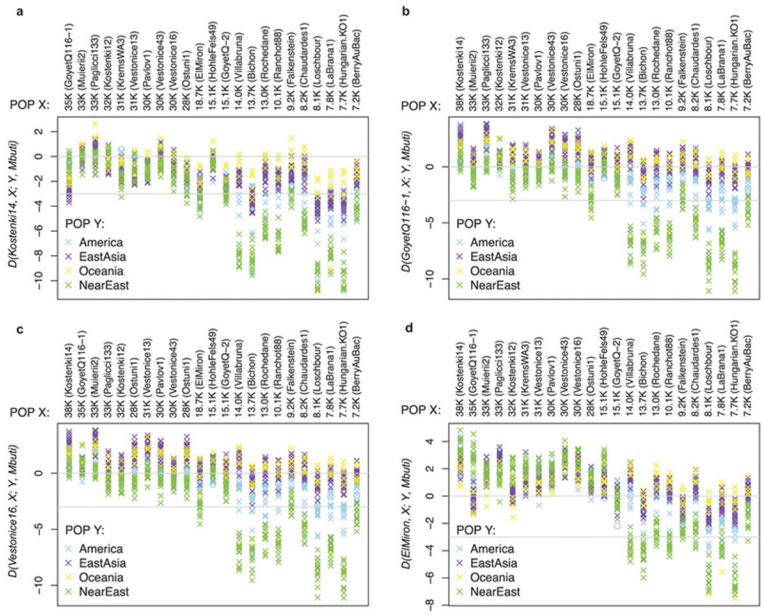

Extended Data Fig. 3. Studying how the relatedness of non-European populations to pairs of European hunter-gatherers changes over time

We examine statistics of the form *D(W, X; Y, Mbuti)*, with the Z-score given on the y-axis, where W is an early European hunter-gatherer, X is another European hunter-gatherer (in chronological order on the x-axis), and Y is a non-European population (see legend). **A:** W=*Kostenki14*. **B:** W=*GoyetQ116-1*. **C:** W=*Vestonice16*. **D:** W=*ElMiron*. |Z|>3 scores are considered statistically significant (horizontal line). The similar Figure 4b gives absolute *D*-statistic values rather than *Z*-scores (for W=*Kostenki14*) and uses pooled regions rather than individual populations Y.

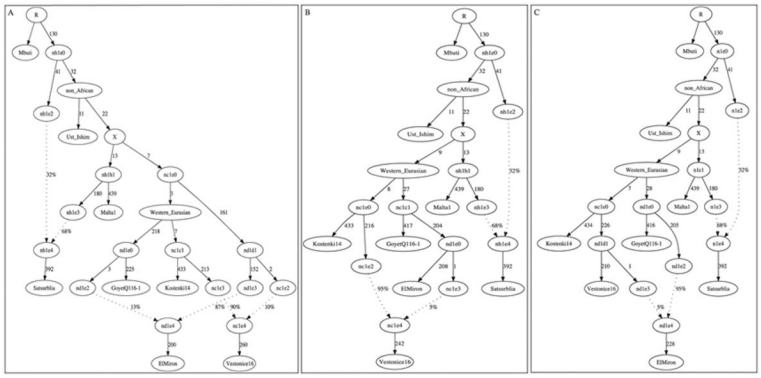

Extended Data Figure 4. An Admixture Graph model that fits the data for *Satsurblia*, an Upper Paleolithic sample from the Caucasus

This model uses 127,057 SNPs covered in all populations. Estimated genetic drifts are give along the solid lines in units of f_2-distance (parts per thousand), and estimated mixture proportions are given along the dotted lines. All three models provide an fit to the allele frequency correlation data among *Mbuti*, *UstIshim*, *Kostenki14*, *Vestonice16*, *Malta1*, *ElMiron* and *Satsurblia* to within the limits of our resolution, in the sense that all empirical

f_2-, f_3- and f_4-statistics relating the samples are within three standard errors of the expectation of the model. Models in which *Satsurblia* is modeled as unadmixed cannot be fit.

Extended Data Table 1

The 51 ancient modern humans analyzed in this study

Sample Code	Data source	Country	Lat.	Long.	Cal BP 95.4%	Date type (ref.)	Culture	Remain	SNP Pane
UstIshim	[1]	Russia	57.43	71.10	47,480-42,560	Direct-UF ([1])	Unassigned	Femur	Shotgun
Oase1	[2]	Romania	45.12	21.90	41,640-37,580	Direct-UF ([3])	Unassigned	Mandible	Shotgun
Kostenki14*	New	Russia	51.23	39.30	38,680-36,260	Direct-UF ([4])	Unassigned	Tibia	3.7M
GoyetQ116-1	New	Belgium	50.26	4.28	35,160-34,430	Direct-NotUF ([5])	Aurignacian	Humerus	1240k
Muierii2	New	Romania	45.11	23.46	33,760-32,840	Direct-UF ([6])	Unassigned	Temporal	3.7M
Paglicci133	New	Italy	41.65	15.61	34,580-31,210	Layer ([7])	Gravettian	Tooth	1240k
Cioclovina1	New	Romania	45.35	23.84	33,090-31,780	Direct-UF ([8])	Unassigned	Cranium	1240k
Kostenki12	New	Russia	51.23	39.30	32,990-31,840	Layer ([9])	Unassigned	Cranium	3.7M
KremsWA3	New	Austria	48.41	15.59	31,250-30,690	Layer ([10])	Gravettian	Cranium	1240K
Vestonice13	New	Czech	48.53	16.39	31,070-30,670	Layer ([9])	Gravettian	Femur	3.7M
Vestonice15	New	Czech	48.53	16.39	31,070-30,670	Layer ([9])	Gravettian	Femur	3.7M
Vestonice14	New	Czech	48.53	16.39	31,070-30,670	Layer ([9])	Gravettian	Femur	390k
Pavlov1	New	Czech	48.53	16.39	31,110-29,410	Layer ([9])	Gravettian	Femur	3.7M
Vestonice43	New	Czech	48.53	16.39	30,710-29,310	Layer ([9])	Gravettian	Femur	3.7M
Vestonice16	New	Czech	48.53	16.39	30,710-29,310	Layer ([9])	Gravettian	Femur	3.7M
Ostuni2	New	Italy	40.73	17.57	29,310-28,640	Direct-UF (New)	Gravettian	Femur	3.7M
GoyetQ53-1	New	Belgium	50.26	4.28	28,230-27,720	Direct-NotUF ([5])	Gravettian	Fibula	1240k
Paglicci108	New	Italy	41.65	15.61	28,430-27,070	Layer ([5])	Gravettian	Phalanx	1240k
Ostuni1	New	Italy	40.73	17.57	27,810-27,430	Direct-UF (New)	Gravettian	Tibia	3.7M
GoyetQ376-19	New	Belgium	50.26	4.28	27,720-27,310	Direct-NotUF ([5])	Gravettian	Humerus	1240k
GoyetQ56-16	New	Belgium	50.26	4.28	26,600-26,040	Direct-NotUF ([5])	Gravettian	Fibula	1240k
Malta1	[11]	Russia	52.9	103.5	24,520-24,090	Direct-UF ([11])	Unassigned	Humerus	Shotgun
ElMiron	New	Spain	43.26	−3.45	18,830-18,610	Direct-UF ([5])	Magdalenian	Toe	3.7M
AfontovaGora3	New	Russia	56.05	92.87	16,930-16,490	Layer ([5])	Unassigned	Tooth	3.7M
AfontovaGora2	[11]	Russia	56.05	92.87	16,930-16,490	Direct-UF ([11])	Unassigned	Humerus	Shotgun
Rigney1	New	France	47.23	6.10	15,690-15,240	Direct-NotUF ([12])	Magdalenian	Mandible	1240k
HohleFels49	New	Germany	48.22	9.45	16,000-14,260	Layer ([13])	Magdalenian	Femur	390k
GoyetQ-2	New	Belgium	50.26	4.28	15,230-14,780	Direct-NotUF ([5])	Magdalenian	Humerus	1240k
Brillenhohle	New	Germany	48.24	9.46	15,120-14,440	Direct-UF ([14])	Magdalenian	Cranium	390k
HohleFels79	New	Germany	48.22	9.45	15,070-14,270	Direct-UF ([5])	Magdalenian	Cranium	390k
Burkhardtshohle	New	Germany	48.32	9.35	15,080-14,150	Direct-UF ([15])	Magdalenian	Cranium	1240k
Villabruna	New	Italy	46.15	12.21	14,180-13,780	Direct-UF ([16])	Epigravettian	Femur	3.7M
Bichon	[17]	Switzerland	47.01	6.79	13,770-13,560	Direct-UF ([17])	Azilian	Petrous	Shotgun
Satsurblia	[17]	Georgia	42.24	42.92	13,380-13,130	Direct-UF ([17])	Epigravettian	Petrous	Shotgun
Rochedane	New	France	47.21	6.45	13,090-12,830	Direct-NotUF ([5])	Epipaleolithic	Mandible	1240k
Iboussieres39	New	France	44.29	4.46	12,040-11,410	Direct-NotUF ([5])	Epipaleolithic	Femur	390k

Sample Code	Data source	Country	Lat.	Long.	Cal BP 95.4%	Date type (ref.)	Culture	Remain	SNP Pane
Continenza	New	Italy	41.96	13.54	11,200-10,510	Layer (New)	Mesolithic	Cranium	3.7M
Ranchot88	New	France	47.91	5.43	10,240-9,930	Direct-NotUF ([5])	Mesolithic	Cranium	1240k
LesCloseaux13	New	France	48.52	2.11	10,240-9,560	Direct-NotUF ([18])	Mesolithic	Femur	1240k
Kotias	[17]	Georgia	42.13	43.12	9,890-9,550	Direct-UF ([17])	Mesolithic	Tooth	Shotgun
Falkenstein	New	Germany	48.06	9.04	9,410-8,990	Direct-UF ([19])	Mesolithic	Fibula	390k
Karelia	[20]	Russia	61.65	35.65	8,800-7,950	Layer ([21])	Mesolithic	Tooth	Shotgun
Bockstein	New	Germany	48.33	10.09	8,370-8,160	Layer ([22])	Mesolithic	Tooth	390k
Ofnet	New	Germany	48.49	10.27	8,430-8,060	Layer ([23])	Mesolithic	Tooth	390k
Chaudardes1	New	France	49.24	3.46	8,360-8,050	Direct-NotUF ([5])	Mesolithic	Tibia	1240k
Loschbour	[24]	Luxembourg	49.70	6.24	8,160-7,940	Direct-UF ([24])	Mesolithic	Tooth	Shotgun
LaBrana1	[25]	Spain	42.93	−5.35	7,940-7,690	Direct-UF ([26])	Mesolithic	Tooth	Shotgun
Hungarian.KO1	[27]	Hungarian	47.93	21.20	7,730-7,590	Direct-UF ([27])	Neolithic	Petrous	Shotgun
Motala12	[24]	Sweden	58.54	15.05	7,670-7,580	Direct-UF (New)	Mesolithic	Tooth	Shotgun
BerryAuBac	New	France	49.24	3.54	7,320-7,170	Direct-NotUF ([5])	Mesolithic	Radius	1240k
Stuttgart	[24]	Germany	48.78	9.18	7,260-7,020	Direct-UF (New)	Early Neolithic	Tooth	Shotgun

Note: All dates are obtained as described in Supplementary Information section 1. When an individual has a direct date from an element from the same skeleton it is marked “Direct”, followed by a hyphen to indicate whether the date is obtained by ultrafiltration (“UF”) or without (“NotUF”). If the date is from the archaeological layers, we mark the date type as “Layer”. All the dates were calibrated using IntCal13[28] and the OxCal4.2 program[29].

[*] We represent Kostenki14 in most analyses by our newly reported 16.1x capture data, but repeat key analyses on the previously reported 2.8x shotgun data[30].

[+] Mean coverage is computed on the 3.7M SNP targets.

Extended Data Table 2

Estimated proportion of Neanderthal ancestry

			f_4-ratios		Archaic Ancestry Informative SNPs				
Sample Code	Age BP	SNPs	Est.	95% CI	SNPs	Est.	95% CI	Increase in Neanderthal ancestry with B	S.E.
UstIshim	45,020	2,137,615	4.4%	3.6% – 5.3%	778,774	3.0%	2.3% – 3.7%	−0.9%	1.3%
Oase1	39,610	285,076	9.9%	8.4% – 11.4%	59,854	7.5%	6.0% – 8.9%	2.5%	1.8%
Kostenki14	37,470	1,774,156	3.6%	2.7% – 4.4%	632,748	2.8%	2.3% – 3.3%	−1.0%	1.0%
GoyetQ116-1	34,795	846,983	3.4%	2.4% – 4.3%					
Muierii2	33,300	98,618	5.2%	3.0% – 7.4%	22,189	3.0%	2.5% – 3.5%	0.6%	1.1%
Paglicci133	32,895	82,330	4.1%	2.1% – 6.0%					
Cioclovina1	32,435	12,784	4.1%	−1.1% – 9.3%					
Kostenki12	32,415	61,228	1.9%	−0.7% – 4.4%	13,385	2.6%	2.1% – 3.2%	1.7%	1.5%
KremsWA3	30,970	203,986	3.9%	2.6% – 5.2%			-		
Vestonice13	30,870	139,568	4.6%	2.6% – 6.5%	35,983	3.3%	2.7% – 3.8%	0.3%	1.3%
Vestonice15	30,870	30,900	4.3%	0.6% – 7.9%	5,855	2.7%	2.1% – 3.4%	−1.5%	1.3%
Vestonice14	30,870	5,677	2.6%	−5.9% – 11.0%					
Pavlov1	30,260	57,005	4.4%	1.6% – 7.1%	9,327	3.1%	2.5% – 3.8%	0.7%	1.2%
Vestonice43	30,010	163,946	6.9%	5.2% – 8.5%	38,749	2.9%	2.4% – 3.3%	0.9%	0.9%

		f_4-ratios			Archaic Ancestry Informative SNPs				
Sample Code	**Age BP**	**SNPs**	**Est.**	**95% CI**	**SNPs**	**Est.**	**95% CI**	**Increase in Neanderthal ancestry with B**	**S.E.**
Vestonice16	30,010	945,292	4.1%	3.1% – 5.1%	268,157	2.8%	2.3% – 3.3%	−0.1%	1.0%
Ostuni2	28,975	17,017	1.6%	−3.2% – 6.3%	2,746	2.3%	1.4% – 3.1%	1.3%	1.6%
GoyetQ53-1	27,975	12,567	4.8%	−0.7% – 10.3%					
Paglicci108	27,750	4,330	3.4%	−6.0% – 12.7%					
Ostuni1	27,620	369,313	4.2%	3.0% – 5.4%	88,449	2.6%	2.2% – 3.0%	0.1%	0.9%
GoyetQ376-19	27,515	25,400	6.5%	2.7% – 10.2%					
GoyetQ56-16	26,320	9,988	3.6%	−1.9% – 9.1%					
Malta1	24,305	1,439,501	2.9%	1.9% – 3.8%	437,187	2.5%	2.1% – 2.9%	1.0%	0.8%
ElMiron	18,720	797,714	3.6%	2.6% – 4.5%	250,071	2.8%	2.5% – 3.2%	0.6%	0.9%
AfontovaGora3	16,710	286,355	3.0%	1.8% – 4.2%	96,237	3.3%	2.9% – 3.7%	−1.5%	1.0%
AfontovaGora2	16,710	143,751	2.2%	0.4% – 4.0%	37,280	2.3%	1.9% – 2.7%	−0.3%	0.9%
Rigney1	15,465	35,600	0.8%	−2.6% – 4.2%					
HohleFels49	15,130	63,151	2.3%	−0.6% – 5.2%					
GoyetQ-2	15,005	72,263	1.7%	−0.6% – 4.0%					
Brillenhohle	14780	13,459	2.5%	−3.0% – 8.1%					
HohleFels79	14,670	11,211	1.7%	−5.1% – 8.5%					
Burkhardtshohle	14,615	38,376	1.7%	−1.6% – 5.0%					
Villabruna	13,980	1,215,433	2.7%	1.8% – 3.5%	425,148	3.3%	3.0% – 3.7%	1.1%	0.9%
Bichon	13,665	2,116,782	2.9%	1.9% – 3.8%	769,422	2.7%	2.2% – 3.2%	0.7%	1.3%
Satsurblia	13,255	1,460,368	1.5%	0.6% – 2.4%	542,561	2.0%	1.7% – 2.4%	0.9%	0.6%
Rochedane	12,960	237,390	1.9%	0.5% – 3.3%					
Iboussieres39	11,725	9,659	6.4%	−0.8% – 13.7%					
Continenza	10,855	11,717	4.1%	−1.4% – 9.6%	1,733	2.9%	1.8% – 4.0%	−10.6%	4.4%
Ranchot88	10,085	414,863	2.9%	1.8% – 4.0%					
LesCloseaux13	9,900	8,635	−3.0%	−9.7% – 3.8%					
Kotias	9,720	2,133,968	1.8%	1.0% – 2.7%	779,146	2.1%	1.8% – 2.4%	0.7%	0.5%
Falkenstein	9,200	64,428	4.8%	1.7% – 7.8%					
Karelia	8,375	1,754,410	1.9%	1.1% – 2.7%	582,444	2.2%	1.9% – 2.6%	−0.2%	0.7%
Bockstein	8,265	21,977	5.7%	1.0% – 10.5%					
Ofnet	8,245	6,263	9.8%	1.4% – 18.1%					
Chaudardes1	8,205	92,657	1.9%	−0.2% – 3.9%					
Loschbour	8,050	2,091,584	2.5%	1.6% – 3.3%	774,139	2.6%	2.0% – 3.1%	2.7%	1.7%
LaBrana1	7,815	1,884,745	1.9%	1.1% – 2.8%	642,231	2.7%	2.3% – 3.2%	0.4%	0.8%
Hungarian.KO1	7,660	1,410,303	2.1%	1.2% – 3.0%	439,408	2.4%	2.0% – 2.8%	−0.1%	1.2%
Motala12	7,625	1,874,519	2.5%	1.6% – 3.3%	655,685	2.3%	1.9% – 2.7%	−0.1%	0.7%
BerryAuBac	7,245	54,690	2.5%	−0.2% – 5.1%					
Stuttgart	7,140	2,078,724	1.9%	1.1% – 2.7%	767,813	2.1%	1.8% – 2.5%	0.0%	0.7%
Dai	0	2,144,502	1.4%	0.7% – 2.1%	782,066	1.8%	1.5% – 2.1%	1.4%	0.4%
Han	0	2,144,502	1.8%	1.1% – 2.5%	782,164	2.1%	1.8% – 2.5%	1.9%	0.7%

		f_4-ratios			Archaic Ancestry Informative SNPs				
Sample Code	**Age BP**	**SNPs**	**Est.**	**95% CI**	**SNPs**	**Est.**	**95% CI**	**Increase in Neanderthal ancestry with B**	**S.E.**
English	0	2,144,502	1.5%	0.8% – 2.2%					
French	0	2,144,502	1.5%	0.9% – 2.1%	782,386	1.7%	1.4% – 1.9%	1.4%	0.6%
Sardinian	0	2,144,502	1.2%	0.6% – 1.9%	782,351	1.7%	1.4% – 2.0%	0.7%	0.5%
Karitiana	0				782,037	2.1%	1.7% – 2.4%	1.5%	1.0%

Extended Data Table 3

Significant correlation of Neanderthal ancestry estimate with specimen age

				Estimate of Neanderthal ancestry at different time points			
Subset of samples	**N**	**P-value for date correlation**	**Decrease in ancestry per 10,000 years**	**0 years ago (present)**	**50,000 years ago**	**55,000 years ago**	**60,000 years ago**
f_4-ratio estimates							
Core Set 1 (all ancient samples (except *Oase1*) + *Han* + *Dai)*	57	5×10^{-22}	0.48–0.73%	1.1–2.2%	4.0–5.4%	4.3–5.7%	4.5–6.0%
Subset of Core Set 1 (<32kya)	50	2×10^{-15}	0.59–0.98%	0.9–2.1%	4.5–6.4%	4.8–6.9%	5.1–7.4%
Subset of Core Set 1 (>32kya or <25kya)	44	4×10^{-18}	0.44–0.69%	1.0–2.2%	3.7–5.2%	4.0–5.5%	4.2–5.8%
Subset of Core Set 1 (>25kya or <14kya)	47	5×10^{-21}	0.48–0.73%	1.0–2.2%	3.9–5.3%	4.2–5.7%	4.5–6.0%
Subset of Core Set 1 (>14kya or present day)	37	2×10^{-18}	0.47–0.74%	1.1–2.4%	4.1–5.5%	4.3–5.8%	4.6–6.2%
Subset of Core Set 1 (only ancient samples)	50	4×10^{-15}	0.46–0.76%	1.0–2.3%	4.0–5.4%	4.3–5.8%	4.5–6.1%
Subset of Core Set 1 (individuals with >200,000 SNPs)	28	4×10^{-19}	0.46–0.71%	1.1–2.3%	3.9–5.3%	4.2–5.7%	4.4–6.0%
Modification of Core Set 1 (replace East Asians with Europeans)	58	2×10^{-23}	0.49–0.73%	1.1–2.3%	4.0–5.4%	4.3–5.8%	4.6–6.1%
All ancient samples including *Oase1* + *Han* + *Dai*	58	8×10^{-29}	0.57–0.81%	1.0–2.2%	4.3–5.7%	4.7–6.1%	5.0–6.5%
All ancient samples	51	1×10^{-20}	0.57–0.86%	0.9–2.2%	4.4–5.8%	4.7–6.2%	5.0–6.6%
All ancient samples except *Oase1* or *UstIshim*	49	8×10^{-12}	0.45–0.81%	1.0–2.3%	4.0–5.6%	4.2–6.0%	4.5–6.4%
Ancestry informative SNPs							
Core Set 2 (all ancient samples (except *Oase1)* + *Han* + *Dai* + *Karitiana)*	29	4×10^{-11}	0.21–0.39%	1.8–2.3%	3.1–4.0%	3.2–4.2%	3.3–4.3%
Subset of Core Set 2 (no *Han, Dai, Karitiana, Stuttgart*)	25	1×10^{-4}	0.11–0.36%	1.8–2.5%	2.9–3.8%	3.0–4.0%	3.0–4.1%
Subset of Core Set 2 (no *Han, Dai, Karitiana, Stuttgart, UstIshim*)	24	2×10^{-4}	0.11–0.37%	1.8–2.5%	2.9–3.8%	2.9–4.0%	3.0–4.2%

Note: The "Core Set 1," used for the *f4*-ratio analyses, refers to 50 ancient samples (removing *Oase1* as an outlier) along with 7 East Asians (*Dai* and *Han*). "Core Set 2," used for the analyses of Neanderthal ancestry informative SNPs, refers to 26 ancient samples (removing *Oase1)* along with *Han*, *Dai*, and *Karitiana*

Extended Data Table 4

Sex determination for newly reported samples.Y-rate is the ratio of N_Y/N_{auto} divided by the same quantity for the genome-wide target set. Female sex (F) is inferred as Y-rate<0.05 and male sex (M) as Y-rate>0.

Sample	Target	Type	N_{auto}	N_X	N_Y	N_X/N_{auto}	N_Y/N_{auto}	X-rate	Y-rate	Sex
	1240k or 2.2M*		1151240	49711	32681	0.0432	0.0284			
	390k		388745	1819	2242	0.0047	0.0058			
Kostenki14	2.2M	all	29633405	395534	262846	0.0133	0.0089	0.309	0.312	M
GoyetQ116-1	1240k	all	2122620	36391	22256	0.0171	0.0105	0.397	0.369	M
Cioclovina1	1240k	Damage	11521	184	125	0.0160	0.0108	0.370	0.382	M
Kostenki12	2.2M	Subset	63908	856	504	0.0134	0.0079	0.310	0.278	M
Muierii2	2.2M	Damage	81165	2177	8	0.0268	0.0001	0.621	0.003	F
Vestonice13	2.2M	Damage	119094	1578	1059	0.0133	0.0089	0.307	0.313	M
Vestonice15	2.2M	Damage	28762	338	227	0.0118	0.0079	0.272	0.278	M
Vestonice14	390k	Damage	4846	8	11	0.0017	0.0023	0.353	0.394	M
Vestonice43	2.2M	Damage	136933	1826	1204	0.0133	0.0088	0.309	0.310	M
Pavlov1	2.2M	Damage	54429	631	404	0.0116	0.0074	0.268	0.261	M
Vestonice16	2.2M	Subset	2433741	30463	20976	0.0125	0.0086	0.290	0.304	M
KremsWA3	1240k	all	235069	4119	2661	0.0175	0.0113	0.406	0.399	M
Ostuni2	2.2M	Damage	15749	138	1	0.0088	0.0001	0.203	0.002	F
Ostuni1	2.2M	Damage	427199	10868	47	0.0254	0.0001	0.589	0.004	F
Paglicci108	1240k	Damage	3883	124	2	0.0319	0.0005	0.740	0.018	F
GoyetQ53-1	1240k	Damage	10771	311	4	0.0289	0.0004	0.669	0.013	F
GoyetQ376-19	1240k	Damage	20052	680	10	0.0339	0.0005	0.785	0.018	F
GoyetQ56-16	1240k	Damage	8702	304	7	0.0349	0.0008	0.809	0.028	F
Paglicci133	1240k	Subset	81092	1641	983	0.0202	0.0121	0.469	0.427	M
ElMiron	2.2M	Damage	1765696	40647	196	0.0230	0.0001	0.533	0.004	F
HohleFels79	390k	Damage	10188	28	22	0.0027	0.0022	0.587	0.374	M
AfontovaGora3	2.2M	Damage	291798	8705	37	0.0298	0.0001	0.691	0.004	F
HohleFels49	390k	Damage	61051	113	111	0.0019	0.0018	0.396	0.315	M
Rigney1	1240k	Damage	32797	1131	9	0.0345	0.0003	0.799	0.010	F
GoyetQ-2	1240k	Damage	65563	1123	706	0.0171	0.0108	0.397	0.379	M
Brillenhohle	390k	Damage	12603	22	22	0.0017	0.0017	0.373	0.303	M
Burkhardtshohle	1240k	Damage	34207	563	407	0.0165	0.0119	0.381	0.419	M
Villabruna	2.2M	Subset	5505838	72055	52110	0.0131	0.0095	0.303	0.333	M
Rochedane	1240k	Subset	256325	4780	2830	0.0186	0.0110	0.432	0.389	M
Continenza	2.2M	Damage	10647	208	2	0.0195	0.0002	0.452	0.007	F
Iboussieres39	390k	Damage	8246	12	22	0.0015	0.0027	0.311	0.463	M
Ranchot88	1240k	Damage	594962	18520	119	0.0311	0.0002	0.721	0.007	F
LesCloseaux13	1240k	Damage	7326	275	2	0.0375	0.0003	0.869	0.010	F
Falkenstein	390k	Damage	58970	113	102	0.0019	0.0017	0.410	0.300	M

Sample	Target	Type	N_{auto}	N_X	N_Y	N_X/N_{auto}	N_Y/N_{auto}	X-rate	Y-rate	Sex
Bockstein	390k	Damage	20214	62	0	0.0031	0.0000	0.655	0.000	F
Ofnet	390k	Damage	5294	13	1	0.0025	0.0002	0.525	0.033	F
Chaudardes1	1240k	Damage	84052	1429	865	0.0170	0.0103	0.394	0.363	M
BerryAuBac	1240k	All	49670	902	554	0.0182	0.0112	0.421	0.393	M

*We restrict analysis to the 1240k target set for study of the 2.2M capture datasets.

Extended Data Table 5

Allele counts at SNPs thought to be affected by selection in samples that have at least 1.0-fold coverage.rs4988235 is responsible for lactase persistence in Europe[59,60]. The SNPs at *SLC24A5* and *SLC45A2* are responsible for light skin pigmentation. The SNP at *EDAR*[61,62] affects tooth morphology and hair thickness. The SNP at *HERC2*[63,64] is the primary determinant of light eye color in present-day Europeans. We present the fraction of fragments overlapping each SNP that are derived; the observation of a low rate of derived alleles does not prove that the individual carried the allele, and instead may reflect sequencing error or ancient DNA damage. We highlight in light gray sites that we judge (based on the derived allele count) are likely to be heterozygous for the derived allele, and in dark gray sites that are likely to be homozygous.

		LCT	*SLC45A2*	*SLC24A5*	*EDAR*	*HERC2*
	SNP	**rs4988235**	**rs16891982**	**rs1426654**	**rs3827760**	**rs12913832**
	Ancestral	G	C	G	A	A
	Derived	A	G	A	G	G
UstIshim	Coverage	31	46	52	42	50
	Derived allele frequency	0%	0%	2%	0%	0%
Kostenki14	Coverage	140	113	6	45	52
	Derived allele frequency	0%	2%	17%	0%	0%
GoyetQ116-1	Coverage	8	6	0	9	1
	Derived allele frequency	0%	0%	n/a	0%	0%
Vestonice16	Coverage	13	18	0	4	5
	Derived allele frequency	0%	6%		0%	0%
Malta1	Coverage	1	0	2	2	2
	Derived allele frequency	0%		0%	0%	0%
ElMiron	Coverage	2	10	0	7	5
	Derived allele frequency	0%	0%		0%	0%
Villabruna	Coverage	17	52	5	19	10
	Derived allele frequency	0%	0%	0%	0%	100%
Bichon	Coverage	11	4	25	16	9
	Derived allele frequency	0%	0%	0%	0%	33%
Satsurblia	Coverage	1	2	4	1	4

		LCT	*SLC45A2*	*SLC24A5*	*EDAR*	*HERC2*
	SNP	**rs4988235**	**rs16891982**	**rs1426654**	**rs3827760**	**rs12913832**
	Derived allele frequency	0%	0%	100%	0%	50%
Kotias	Coverage	16	22	13	20	15
	Derived allele frequency	0%	0%	100%	0%	0%
Loschbour	Coverage	19	18	20	17	21
	Derived allele frequency	0%	0%	0%	0%	100%
LaBrana1	Coverage	8	6	2	11	3
	Derived allele frequency	12%	0%	0%	0%	100%
Hungarian.KO1	Coverage	1	2	2	1	2
	Derived allele frequency	0%	0%	50%	0%	100%
Motala12	Coverage	2	0	3	3	1
	Derived allele frequency	0%		0%	33%	100%
Karelia	Coverage	1	9	4	0	1
	Derived allele frequency	0%	67%	0%		0%
Stuttgart	Coverage	25	21	15	29	21
	Derived allele frequency	0%	0%	100%	0%	0%

Extended Data Table 6

All European hunter-gatherers after Kostenki14 share genetic drift with present-day Europeans.We compute the statistic *D(Han, Test; French, Mbuti)*. Measuring whether present-day *French* share more alleles with *Han* or with a *Test* population (restricting to ancient samples with at least 30,000 SNPs covered at least once). Present-day Europeans share significantly more genetic drift with European hunter-gatherers from *Kostenki14* onward than they do with *Han*. Thus, by the date of *Kostenki14*, there was already West Eurasian-specific genetic drift.

Test	**SNPs used**	**D-value**	**Z score**
Ust'-Ishim	2,050,358	0.003	6.6
Oase1	278,785	0.005	10.6
Kostenki14	1,676,253	−0.002	−5.5
Muierii2	95,787	−0.004	−6.3
GoyetQ116-1	811,756	−0.004	−8.0
Kostenki12	59,850	−0.004	−5.1
Paglicci133	79,624	−0.004	−5.5
Vestonice13	136,598	−0.004	−7.1
Vestonice15	30,252	−0.006	−6.4
Vestonice16	914,141	−0.004	−9.1
Pavlov1	55,835	−0.005	−6.3

Test	SNPs used	D-value	Z score
Vestonice43	160,463	−0.004	−6.9
KremsWA3	229,187	−0.005	−10.2
Ostuni1	360,347	−0.004	−8.6
Malta1	1,401,718	−0.005	−11.3
ElMiron	777,654	−0.007	−14.7
AfontovaGora2	141,073	−0.007	−13.6
AfontovaGora3	707,617	−0.006	−13.6
HohleFels49	62,816	−0.004	−5.2
Rigney1	34,445	−0.006	−6.1
GoyetQ-2	70,210	−0.006	−8.8
Burkhardtshohle	37,234	−0.006	−6.2
Villabruna	1,170,777	−0.010	−24.7
Bichon	2,034,069	−0.009	−23.6
Satsurblia	1,419,824	−0.005	−13.1
Rochedane	229,806	−0.011	−20.8
Ranchot88	402,274	−0.010	−21.8
Kotias	2,047,856	−0.006	−15.8
Falkenstein	64,043	−0.008	−11.6
Chaudardes1	90,047	−0.011	−16.0
Loschbour	2,037,082	−0.011	−25.4
LaBrana1	1,824,307	−0.009	−23.0
Motala12	1,816,201	−0.009	−23.8
Hungarian.KO1	1,372,801	−0.010	−26.5
Karelia	1,701,664	−0.009	−21.9
Stuttgart	2,023,939	−0.009	−23.9
BerryAuBac	53,028	−0.011	−14.0

Supplementary Material

Refer to Web version on PubMed Central for supplementary material.

Authors

Qiaomei Fu[1,2,3], Cosimo Posth[4,5,*], Mateja Hajdinjak[3,*], Martin Petr[3], Swapan Mallick[2,6,7], Daniel Fernandes[8,9], Anja Furtwängler[4], Wolfgang Haak[5,10], Matthias Meyer[3], Alissa Mittnik[4,5], Birgit Nickel[3], Alexander Peltzer[4], Nadin Rohland[2], Viviane Slon[3], Sahra Talamo[11], Iosif Lazaridis[2], Mark Lipson[2], Iain Mathieson[2], Stephan Schiffels[5], Pontus Skoglund[2], Anatoly P. Derevianko[12,13], Nikolai Drozdov[12], Vyacheslav Slavinsky[12], Alexander Tsybankov[12], Renata Grifoni Cremonesi[14], Francesco Mallegni[15], Bernard Gély[16], Eligio Vacca[17], Manuel R. González Morales[18], Lawrence G. Straus[18,19], Christine Neugebauer-Maresch[20], Maria Teschler-Nicola[21,22], Silviu Constantin[23], Oana Teodora Moldovan[24], Stefano Benazzi[11,25], Marco Peresani[26], Donato Coppola[27,28], Martina Lari[29], Stefano

Ricci[30], Annamaria Ronchitelli[30], Frédérique Valentin[31], Corinne Thevenet[32], Kurt Wehrberger[33], Dan Grigorescu[34], Hélène Rougier[35], Isabelle Crevecoeur[36], Damien Flas[37], Patrick Semal[38], Marcello A. Mannino[11,39], Christophe Cupillard[40,41], Hervé Bocherens[42,43], Nicholas J. Conard[43,44], Katerina Harvati[43,45], Vyacheslav Moiseyev[46], Dorothée G. Drucker[42], Jiří Svoboda[47,48], Michael P. Richards[11,49], David Caramelli[29], Ron Pinhasi[8], Janet Kelso[3], Nick Patterson[6], Johannes Krause[4,5,43,+], Svante Pääbo[3,+], and David Reich[2,6,7,+]

Affiliations

[1]Key Laboratory of Vertebrate Evolution and Human Origins of Chinese Academy of Sciences, IVPP, CAS, Beijing 100044, China [2]Department of Genetics, Harvard Medical School, Boston, Massachusetts 02115, USA [3]Department of Evolutionary Genetics, Max Planck Institute for Evolutionary Anthropology, Leipzig 04103, Germany [4]Institute for Archaeological Sciences, Archaeo- and Palaeogenetics, University of Tübingen, Tübingen 72070, Germany [5]Max Planck Institute for the Science of Human History, 07745 Jena, Germany [6]Broad Institute of MIT and Harvard, Cambridge Massachusetts 02142, USA [7]Howard Hughes Medical Institute, Harvard Medical School, Boston, Massachusetts 02115, USA [8]School of Archaeology and Earth Institute, Belfield, University College Dublin, Dublin 4, Ireland [9]CIAS, Department of Life Sciences, University of Coimbra, 3000-456 Coimbra, Portugal [10]Australian Centre for Ancient DNA, School of Biological Sciences, The University of Adelaide, SA-5005 Adelaide, Australia [11]Department of Human Evolution, Max Planck Institute for Evolutionary Anthropology, 04103 Leipzig, Germany [12]Institute of Archaeology and Ethnography, Russian Academy of Sciences, Siberian Branch, 17 Novosibirsk, RU-630090, Russia [13]Altai State University, Barnaul, RU-656049, Russia [14]Dipartimento di Civiltà e Forme del Sapere, Università di Pisa, 56126 Pisa, Italy [15]Department of Biology, University of Pisa 56126 Pisa, Italy [16]Direction régionale des affaires culturelles Rhône-Alpes, 69283 Lyon cedex 01, France [17]Dipartimento di Biologia, Università degli Studi di Bari ‘Aldo Moro’, 70125 Bari, Italy [18]Instituto Internacional de Investigaciones Prehistoricas, Universidad de Cantabria, 39005 Santander, Spain [19]Department of Anthropology MSC01 1040, University of New Mexico, Albuquerque, NM 87131-0001, USA [20]Quaternary Archaeology, Institute for Institute for Oriental and European Archaeology, Austrian Academy of Sciences, 1010 Vienna, Austria [21]Department of Anthropology, Natural History Museum Vienna, 1010 Vienna, Austria [22]Department of Anthropology, University of Vienna, 1090 Vienna, Austria [23]“Emil Racovita” Institute of Speleology, 010986 Bucharest 12, Romania [24]“Emil Racovita” Institute of Speleology, Cluj Branch, 400006 Cluj, Romania [25]Department of Cultural Heritage, University of Bologna, Ravenna, 48121, Italy [26]Sezione di Scienze Preistoriche e Antropologiche, Dipartimento di Studi Umanistici, Università di Ferrara, 44100 Ferrara, Italy [27]Università degli Studi di Bari ‘Aldo Moro’, 70125 Bari, Italy [28]Museo di “Civiltà preclassiche della Murgia meridionale”, 72017 Ostuni, Italy [29]Dipartimento di Biologia, Università di Firenze, 50122 Florence, Italy [30]Dipartimento di Scienze Fisiche, della Terra e dell’Ambiente, U.R. Preistoria e Antropologia, Università degli Studi di Siena, 53100 Siena, Italy [31]CNRS/ UMR

7041 ArScAn MAE, 92023 Nanterre, France [32]INRAP/ UMR 8215 Trajectoires 21, 92023 Nanterre, France [33]Ulmer Museum, 89073 Ulm, Germany [34]University of Bucharest, Faculty of Geology and Geophysics, Department of Geology, 01041 Bucharest, Romania [35]Department of Anthropology, California State University Northridge, Northridge, CA 91330-8244, USA [36]Université de Bordeaux, CNRS, UMR 5199-PACEA, 33615 Pessac Cedex, France [37]TRACES – UMR 5608, Université Toulouse Jean Jaurès, Maison de la Recherche, 31058 Toulouse Cedex 9, France [38]Royal Belgian Institute of Natural Sciences, 1000 Brussels, Belgium [39]Department of Archaeology, School of Culture and Society, Aarhus University, 8270 Højbjerg, Denmark [40]Service Régional d'Archéologie de Franche-Comté, 25043 Besançon Cedex, France [41]Laboratoire de Chrono-Environnement, UMR 6249 du CNRS, UFR des Sciences et Techniques, 25030 Besançon Cedex, France [42]Department of Geosciences, Biogeology, University of Tübingen, 72074 Tübingen, Germany [43]Senckenberg Centre for Human Evolution and Palaeoenvironment, University of Tübingen, 72072 Tübingen, Germany [44]Department of Early Prehistory and Quaternary Ecology, University of Tübingen, 72070 Tübingen, Germany [45]Institute for Archaeological Sciences, Paleoanthropology, University of Tübingen, 72070 Tübingen, Germany [46]Museum of Anthropology and Ethnography, Saint Petersburg 34, Russia [47]Department of Anthropology, Faculty of Science, Masaryk University, 611 37 Brno, Czech Republic [48]Institute of Archaeology at Brno, Academy of Science of the Czech Republic, 69129 Dolní Věstonice, Czech Republic [49]Department of Anthropology, University of British Columbia, Vancouver, British Columbia V6T 1Z1, Canada

Acknowledgments

We thank Bridget Alex, David Meltzer, Priya Moorjani, Iñigo Olalde, Sriram Sankararaman and Bence Viola for critical comments, Kristin Stewardson and Eadaoin Harney for sample screening, and Fredrik Hallgren for sharing a radiocarbon date for *Motala12*. The Figure 1 map is plotted using data available under the Open Database License © OpenStreetMap (www.openstreetmap.org/copyright). The Goyet project led by HR was funded by the Wenner-Gren Foundation (Gr. 7837), the College of Social and Behavioral Sciences of CSUN, and the RBINS. The excavation of the El Mirón Cave burial, led by LGS and MRGM, was supported by the Gobierno de Cantabria, the L.S.B. Leakey Foundation, the University of New Mexico, the Stone Age Research Fund (J. and R. Auel, principal donors), the town of Ramales de la Victoria and the Universidad de Cantabria. Excavations at Grotta Paglicci were performed by Professor A. Palma di Cesnola in collaboration with the Soprintendenza Archeologia della Puglia (founded by MIUR and local Institutions). Research at Riparo Villabruna was supported by MIBACT and the Veneto Region. QF was funded by the Special Foundation of the President of the Chinese Academy of Sciences (2015–2016), the Bureau of International Cooperation of Chinese Academy of Sciences, Chinese Academy of Sciences (XDA05130202), the National Natural Science Foundation of China (L1524016) and the Chinese Academy of Sciences Discipline Development Strategy Project (2015-DX-C-03). DFe was supported by an Irish Research Council grant (GOIPG/2013/36). IM was supported by a long-term fellowship from the Human Frontier Science Program LT001095/2014-L. PSk was supported by the Swedish Research Council (VR 2014-453). ST, MPR and SP were funded by the Max Planck Society and the Krekeler Foundation. CN-M was funded by FWF P-17258, P-19347, P-21660 and P-23612. SC and OTM were funded by a "Karsthives" Grant PCCE 31/2010 (CNCS-UEFISCDI, Romania). APD, ND, VSla and ND were funded by the Russian Science Foundation (Project No.14-50-00036). MAM was funded by a Marie Curie Intra-European Fellowship within the 7th European Community Framework Programme (grant number PIEF-GA-2008-219965). MLa and DC were funded by grants PRIN 2010-11 and 2010EL8TXP_003. CC and the research about the French Jura sites of Rochedane, Rigney and Ranchot was funded by the Collective Research Program (PCR) (2005–2008). KH was supported by the European Research Council (ERC StG 283503) and the Deutsche Forschungsgemeinschaft (DFG INST37/706-1FUGG, DFG FOR2237). DGD was funded by the European Social Fund and Ministry of Science, Research and Arts of Baden-Württemberg. RP was funded by ERC starting grant ADNABIOARC (263441). JKr was funded by DFG grant KR 4015/1-1, the Baden Württemberg Foundation, and the Max Planck Society. JKe was funded by a grant from the

Deutsche Forschungsgemeinschaft (SFB1052, project A02). DR was funded by NSF HOMINID grant BCS-1032255, NIH (NIGMS) grant GM100233, and the Howard Hughes Medical Institute.

References

1. Gamble C, Davies W, Pettitt P, Richards M. Climate change and evolving human diversity in Europe during the last glacial. Philosophical transactions of the Royal Society of London. Series B, Biological sciences. 2004; 359:24–53. discussion 253–244. DOI: 10.1098/rstb.2003.1396
2. Jones ER, et al. Upper Palaeolithic genomes reveal deep roots of modern Eurasians. Nature communications. 2015; 6:8912.
3. Fu Q, et al. An early modern human from Romania with a recent Neanderthal ancestor. Nature. 2015
4. Seguin-Orlando A, et al. Paleogenomics. Genomic structure in Europeans dating back at least 36,200 years. Science. 2014; 346:1113–1118. DOI: 10.1126/science.aaa0114 [PubMed: 25378462]
5. Dabney J, et al. Complete mitochondrial genome sequence of a Middle Pleistocene cave bear reconstructed from ultrashort DNA fragments. Proc Natl Acad Sci U S A. 2013; 110:15758–15763. DOI: 10.1073/pnas.1314445110 [PubMed: 24019490]
6. Meyer M, Kircher M. Illumina sequencing library preparation for highly multiplexed target capture and sequencing. Cold Spring Harbor protocols. 2010; 2010 pdb prot5448.
7. Meyer M, et al. A High-Coverage Genome Sequence from an Archaic Denisovan Individual. Science. 2012
8. Rohland N, Harney E, Mallick S, Nordenfelt S, Reich D. Partial uracil-DNA-glycosylase treatment for screening of ancient DNA. Philosophical transactions of the Royal Society of London. Series B, Biological sciences. 2015; 370:20130624. [PubMed: 25487342]
9. Haak W, et al. Massive migration from the steppe was a source for Indo-European languages in Europe. Nature. 2015
10. Korneliussen TS, Albrechtsen A, Nielsen R. ANGSD: Analysis of Next Generation Sequencing Data. BMC bioinformatics. 2014; 15:356. [PubMed: 25420514]
11. Krause J, et al. A complete mtDNA genome of an early modern human from Kostenki, Russia. Current biology: CB. 2010; 20:231–236. DOI: 10.1016/j.cub.2009.11.068 [PubMed: 20045327]
12. Skoglund P, et al. Origins and genetic legacy of Neolithic farmers and hunter-gatherers in Europe. Science. 2012; 336:466–469. DOI: 10.1126/science.1216304 [PubMed: 22539720]
13. Fu Q, et al. Genome sequence of a 45,000-year-old modern human from western Siberia. Nature. 2014; 514:445–449. DOI: 10.1038/nature13810 [PubMed: 25341783]
14. Raghavan M, et al. Upper Palaeolithic Siberian genome reveals dual ancestry of Native Americans. Nature. 2014; 505:87–91. DOI: 10.1038/nature12736 [PubMed: 24256729]
15. Lazaridis I, et al. Ancient human genomes suggest three ancestral populations for present-day Europeans. Nature. 2014; 513:409–413. DOI: 10.1038/nature13673 [PubMed: 25230663]
16. Olalde I, et al. Derived immune and ancestral pigmentation alleles in a 7,000-year-old Mesolithic European. Nature. 2014; 507:225–228. DOI: 10.1038/nature12960 [PubMed: 24463515]
17. Gamba C, et al. Genome flux and stasis in a five millennium transect of European prehistory. Nature communications. 2014; 5:5257.
18. Green RE, et al. A draft sequence of the Neandertal genome. Science. 2010; 328:710–722. 328/5979/710 [pii]. DOI: 10.1126/science.1188021 [PubMed: 20448178]
19. Prufer K, et al. The complete genome sequence of a Neanderthal from the Altai Mountains. Nature. 2014; 505:43–49. DOI: 10.1038/nature12886 [PubMed: 24352235]
20. Mallick S. The landscape of human genome diversity. In submission. 2015
21. Reich D, et al. Genetic history of an archaic hominin group from Denisova Cave in Siberia. Nature. 2010; 468:1053–1060. nature09710 [pii]. DOI: 10.1038/nature09710 [PubMed: 21179161]
22. Sankararaman S, et al. The genomic landscape of Neanderthal ancestry in present-day humans. Nature. 2014; 507:354–357. DOI: 10.1038/nature12961 [PubMed: 24476815]
23. Vernot B, Akey JM. Resurrecting surviving Neandertal lineages from modern human genomes. Science. 2014; 343:1017–1021. DOI: 10.1126/science.1245938 [PubMed: 24476670]

24. Harris, K.; Nielsen, R. The Genetic Cost of Neanderthal Introgression. biorxiv.org. 2015. http://dx.doi.org/10.1101/030387
25. Juric, I.; Aeschbacher, S.; Coop, C. The Strength of Selection Against Neanderthal Introgression. biorxiv.org. 2015. http://dx.doi.org/10.1101/030148
26. Posth C, et al. Pleistocene Mitochondrial Genomes Suggest a Single Major Dispersal of Non-Africans and a Late Glacial Population Turnover in Europe. Current Biology.
27. Olivieri A, et al. The mtDNA legacy of the Levantine early Upper Palaeolithic in Africa. Science. 2006; 314:1767–1770. DOI: 10.1126/science.1135566 [PubMed: 17170302]
28. Patterson NJ, et al. Ancient Admixture in Human History. Genetics. 2012
29. Alexander DH, Novembre J, Lange K. Fast model-based estimation of ancestry in unrelated individuals. Genome research. 2009; 19:1655–1664. DOI: 10.1101/gr.094052.109 [PubMed: 19648217]
30. Skotte L, Korneliussen TS, Albrechtsen A. Estimating individual admixture proportions from next generation sequencing data. Genetics. 2013; 195:693–702. DOI: 10.1534/genetics.113.154138 [PubMed: 24026093]
31. Fu Q, et al. A revised timescale for human evolution based on ancient mitochondrial genomes. Curr Biol. 2013; 23:553–559. DOI: 10.1016/j.cub.2013.02.044 [PubMed: 23523248]
32. Conard NJ. A female figurine from the basal Aurignacian of Hohle Fels Cave in southwestern Germany. Nature. 2009; 459:248–252. DOI: 10.1038/nature07995 [PubMed: 19444215]
33. Straus LG. After the Deep Freeze: Confronting “Magdalenian” Realities in Cantabrian Spain And Beyond. Journal of Archaeological Method and Theory. 2013; 20:236–255. DOI: 10.1007/s10816-012-9152-5
34. Weaver AJ, Saenko OA, Clark PU, Mitrovica JX. Meltwater pulse 1A from Antarctica as a trigger of the Bolling-Allerod warm interval. Science. 2003; 299:1709–1713. DOI: 10.1126/science.1081002 [PubMed: 12637739]
35. Montoya C, Peresani M. Bracco JP, Montoya C. Premiers éléments de diachronie dans l’Epigravettien récent des Préalpes de la Vénétie. D’un monde à l’autre. Les systèmes lithiques pendant le Tardiglaciaire autour de la Méditerranée nord-occidentale. Mémoire Societé Préhistorique Française. 2005:123–138.
36. Valentin, B. Paris, Publications de la Sorbonne, Cahiers archéologiques de Paris 1, 1. 2008. Jalons pour une Paléohistoire des derniers chasseurs (XIVe-VIe millénaire avant J.-C.).
37. Pala M, et al. Mitochondrial DNA signals of late glacial recolonization of Europe from near eastern refugia. American journal of human genetics. 2012; 90:915–924. DOI: 10.1016/j.ajhg.2012.04.003 [PubMed: 22560092]
38. McVean G, Awadalla P, Fearnhead P. A coalescent-based method for detecting and estimating recombination from gene sequences. Genetics. 2002; 160:1231–1241. [PubMed: 11901136]
39. Rougier H, et al. Pestera cu Oase 2 and the cranial morphology of early modern Europeans. Proceedings of the National Academy of Sciences of the United States of America. 2007; 104:1165–1170. DOI: 10.1073/pnas.0610538104 [PubMed: 17227863]
40. Marom A, McCullagh JSO, Higham TFG, Sinitsyn AA, Hedges REM. Single amino acid radiocarbon dating of Upper Paleolithic modern humans. Proceedings of the National Academy of Sciences of the United States of America. 2012; 109:6878–6881. DOI: 10.1073/pnas.1116328109 [PubMed: 22517758]
41. Soficaru A, Dobos A, Trinkaus E. Early modern humans from the Pestera Muierii, Baia de Fier, Romania. Proceedings of the National Academy of Sciences of the United States of America. 2006; 103:17196–17201. DOI: 10.1073/pnas.0608443103 [PubMed: 17085588]
42. Palma di Cesnola, A. L’Aurignaziano e il Gravettiano antico. Claudio Grenzi Ed; 2004. Paglicci.
43. Soficaru A, Petrea C, Dobos A, Trinkaus E. The human cranium from the Pestera Cioclovina Uscata, Romania - Context, age, taphonorny, morphology, and paleopathology. Curr Anthropol. 2007; 48:611–619. DOI: 10.1086/519915
44. Trinkaus, E.; Svoboda, J. Early Modern Human Evolution in Central Europe: The People of Dolní Věstonice and Pavlov. Vol. 12. Oxford University Press; 2006.

45. Simon U, Haendel M, Einwoegerer T, Neugebauer-Maresch C. The archaeological record of the Gravettian open air site Krems-Wachtberg. Quaternary International. 2014; 351:5–13. DOI: 10.1016/j.quaint.2013.08.009
46. Cupillard C, et al. Changes in ecosystems, climate and societies in the Jura Mountains between 40 and 8 ka cal BP. Quaternary International. 2015; 378:40–72. DOI: 10.1016/j.quaint.2014.05.032
47. Housley RA, Gamble CS, Street M, Pettitt PB. Radiocarbon evidence for the Lateglacial human recolonisation of Norther Europe. Proc Prehist Soc. 1997; 63:25–54.
48. Benazzi S, et al. Early dispersal of modern humans in Europe and implications for Neanderthal behaviour. Nature. 2011; 479:525–528. DOI: 10.1038/nature10617 [PubMed: 22048311]
49. Simon U. Die Burkhardtshöhle - eine Magdalénienstation am Nordrand der Schwäbischen Alb. Magisterarbeit. 1993
50. Vercellotti G, Alciati G, Richards MP, Formicola V. The Late Upper Paleolithic skeleton Villabruna 1 (Italy): a source of data on biology and behavior of a 14.000 year-old hunter. Journal of Anthropological Sciences. 2008; 86:143–163. [PubMed: 19934473]
51. Valentin F, et al. Découvertes récentes d'inhumations et d'incinération datées du Mésolithique en Ile de France. Revue Archéologique d'Ile-de-France. 2008:21–42.
52. Bramanti B, et al. Genetic discontinuity between local hunter-gatherers and central Europe's first farmers. Science. 2009; 326:137–140. DOI: 10.1126/science.1176869 [PubMed: 19729620]
53. Price TD, Jacobs K. Olenii Ostrov - 1st radiocarbon dates from a major mesolithic cemetery in Karelia, USSR. Antiquity. 1990; 64:849–853.
54. Wehrberger K. Der Streit ward definitiv beendet..." Eine mesolithische Bestattung aus der Bocksteinhöhle im Lonetal, Alb-Donau-Kreis. Zur Erinnerung an Ludwig Bürger (1844–1898). Archäologisches Korrespondenzblatt. 2000; 30:15–31.
55. Orschiedt, J. Dissertation. Vol. 13. Urgeschichtliche Materialhefte; 1999. Manipulationen an menschlichen Skelettresten. Taphonomische Prozesse, Sekundärbestattungen oder Kannibalismus.
56. Sanchez-Quinto F, et al. Genomic affinities of two 7,000-year-old Iberian hunter-gatherers. Curr Biol. 2012; 22:1494–1499. DOI: 10.1016/j.cub.2012.06.005 [PubMed: 22748318]
57. Reimer PJ, et al. Intcal13 and Marine13 Radiocarbon Age Calibration Curves 0–50,000 Years cal BP. Radiocarbon. 2013; 55:1869–1887.
58. Ramsey CB, Lee S. Recent and planned developments of the program OxCal. Radiocarbon. 2013; 55:720–730.
59. Enattah NS, et al. Identification of a variant associated with adult-type hypolactasia. Nature genetics. 2002; 30:233–237. DOI: 10.1038/ng826 [PubMed: 11788828]
60. Bersaglieri T, et al. Genetic signatures of strong recent positive selection at the lactase gene. American journal of human genetics. 2004; 74:1111–1120. DOI: 10.1086/421051 [PubMed: 15114531]
61. Fujimoto A, et al. A scan for genetic determinants of human hair morphology: EDAR is associated with Asian hair thickness. Human molecular genetics. 2008; 17:835–843. DOI: 10.1093/hmg/ddm355 [PubMed: 18065779]
62. Kimura R, et al. A common variation in EDAR is a genetic determinant of shovel-shaped incisors. American journal of human genetics. 2009; 85:528–535. DOI: 10.1016/j.ajhg.2009.09.006 [PubMed: 19804850]
63. Sturm RA, et al. A single SNP in an evolutionary conserved region within intron 86 of the HERC2 gene determines human blue-brown eye color. American journal of human genetics. 2008; 82:424–431. DOI: 10.1016/j.ajhg.2007.11.005 [PubMed: 18252222]
64. Eiberg H, et al. Blue eye color in humans may be caused by a perfectly associated founder mutation in a regulatory element located within the HERC2 gene inhibiting OCA2 expression. Human genetics. 2008; 123:177–187. DOI: 10.1007/s00439-007-0460-x [PubMed: 18172690]

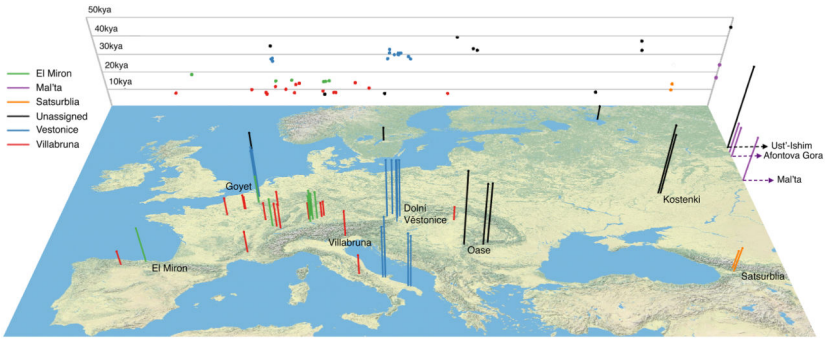

Figure 1. Location and age of 51 ancient samples

Each bar corresponds to a sample, the color code designates the genetically defined sample cluster, and the height is proportional to sample age (the background grid shows a projection of longitude against sample age). To help in visualization, we add jitter for sites with multiple samples from nearby locations. Four samples that are from Siberia are plotted at the far eastern edge of the map.

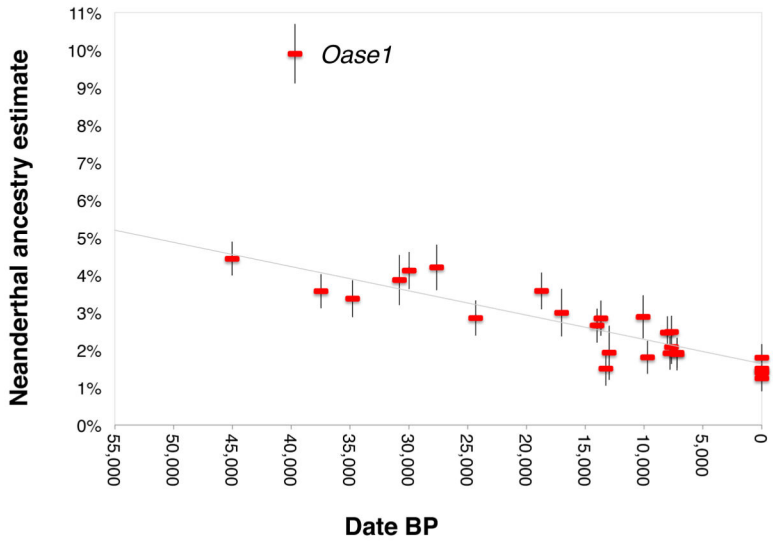

Figure 2. Decrease of Neanderthal ancestry over time

Plot of radiocarbon date against Neanderthal ancestry for samples with at least >200,000 SNPs covered, along with present-day Eurasians (standard errors are from a Block Jackknife). The least squares fit (gray) excludes the data from *Oase1* (an outlier with recent Neanderthal ancestry) and three present-day European populations (known to have less Neanderthal ancestry than East Asians). The slope is significantly negative for all eleven subsets of samples we analyzed ($10^{-29}<P<10^{-11}$ based on a Block Jackknife) (Extended Data Table 3).

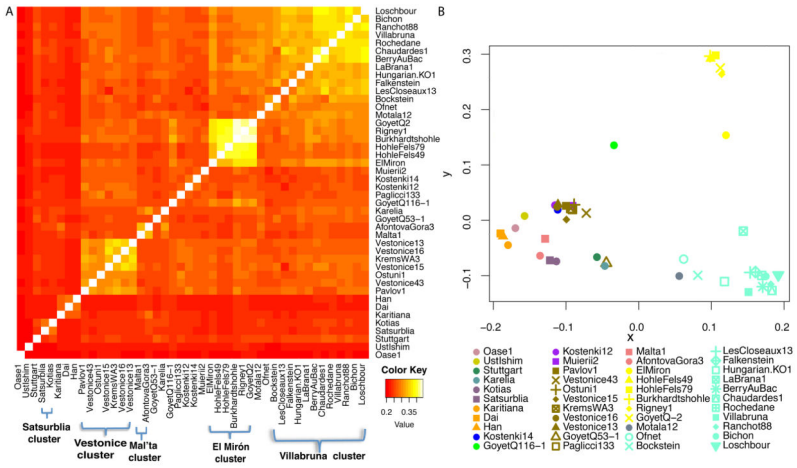

Figure 3. Genetic clustering

(A) Shared genetic drift measured by f_3(X,Y; Mbuti) among samples with at least 30,000 SNPs covered (for AfontovaGora3, ElMiron, Falkenstein, GoyetQ-2, GoyetQ53-1, HohleFels49, HohleFels79, LesCloseaux13, Ofnet, Ranchot88 and Rigney1, we use all sequences for higher resolution). Lighter colors indicate more shared drift. (B) Multidimensional Dimensional Scaling (MDS) analysis, computed using the R software cmdscale package, highlights the main genetic groupings analyzed in this study: Vestonice Cluster (brown), Mal'ta Cluster (pink), El Mirón Cluster (yellow), Villabruna Cluster (light blue), and Satsurblia Cluster (dark purple). The affinity of GoyetQ116-1 (green) to the El Mirón Cluster is evident in both views of the data.

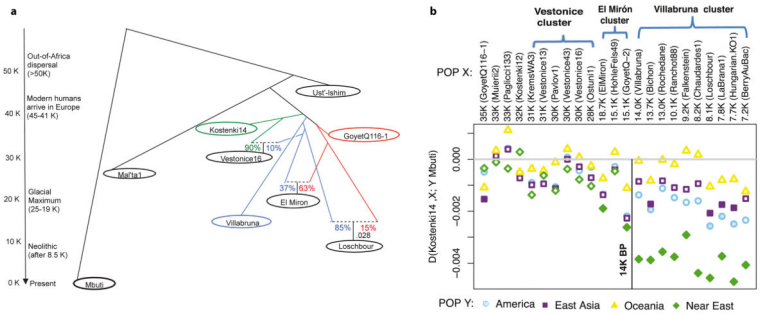

Figure 4. Population history inferences

(A) Admixture Graph relating selected high coverage samples. Dashed lines show inferred admixture events; the estimated mixture proportions fitted using the ADMIXTUREGRAPH software are labeled[28] (the estimated genetic drift on each branch is given in a version of this graph shown in Supplementary Information section 6). The samples are positioned vertically based on their radiocarbon date, but we caution that the population split times are not accurately known. We use color to highlight important early branches of the European founder population: the *Kostenki14* lineage is modeled as the predominant contributor to the Vestonice Cluster (green); the *GoyetQ116-1* lineage as the predominant contributor to the El Mirón Cluster (red); and the *Villabruna* lineage as broadly represented across many clusters. (B) Drawing together of European and Near Eastern populations ~14,000 years ago. Plot of affinity of each pre-Neolithic European population *X* to non-Africans outside Europe *Y* moving forward in time, comparing to *Kostenki14* as a baseline; values Z<-3 standard errors below zero are indicated with filled symbols (we restricted to individuals with >50,000 SNPs). We observe an affinity to Near Easterners beginning with the Villabruna Cluster, and another to East Asians that affects a subset of the Villabruna Cluster.